ChemPubSoc Europe

DOI: 10.1002/chem.201405460

CHEMISTRY
A European Journal
Full Paper

C–H Activation

Rhodium Bis(quinolinyl)benzene Complexes for Methane Activation and Functionalization

Ross Fu,[a] Matthew E. O'Reilly,[b] Robert J. Nielsen,[a] William A. Goddard III ,*[a] and T. Brent Gunnoe*[b]

Abstract: A series of rhodium(III) bis(quinolinyl)benzene (bisq^x) complexes was studied as candidates for the homogeneous partial oxidation of methane. Density functional theory (DFT) (M06 with Poisson continuum solvation) was used to investigate a variety of (bisq^x) ligand candidates involving different functional groups to determine the impact on Rh^{III}(bisq^x)-catalyzed methane functionalization. The free energy activation barriers for methane C–H activation and Rh–methyl functionalization at 298 K and 498 K were determined. DFT studies predict that the best candidate for catalytic methane functionalization is Rh^{III} coordinated to unsubstituted bis(quinolinyl)benzene (bisq). Support is also found for the prediction that the η^2-benzene coordination mode of (bisq^x) ligands on Rh encourages methyl group functionalization by serving as an effective leaving group for S_N2 and S_R2 attack.

Introduction

Methane, the main component of natural gas, is widely abundant. However, owing to its low boiling point of 110 K at standard pressure, it is difficult to store and transport. Methane is also a potent greenhouse gas with 72 times the global warming potential of carbon dioxide, and therefore it cannot be simply released into the atmosphere. Thus, it is often more economical to flare natural gas than to capture and transport it.[1] The amount of methane flared globally is very large (approximately equivalent to the combined natural gas consumption of Central and South America), representing a tremendous amount of wasted energy.[2]

Current industrial processes to utilize surplus methane have centered on using the steam-methane reformation process to convert it to syngas (a CO and H_2 mixture) and then to methanol.[3] However, this process requires very high pressures and temperatures (40 atm, 1000–1400 K), making it both very expensive and energetically demanding. For these reasons, a direct partial oxidation of methane [Eq. (1)], with $\Delta H^\circ = -30$ kcal mol^{-1}, has long been a tempting alternative.

$$CH_4 + {}^1/_2O_2 \rightarrow CH_3OH \qquad (1)$$

However, progress in this direction has been hampered because CH_4 is highly inert with a C–H bond dissociation energy (BDE) of 104 kcal mol^{-1}, whereas the C–H BDE in CH_3OH is only 95 kcal mol^{-1}. Hence, potential oxidation strategies that rely on initial homolytic methane C–H bond dissociation often result in over-oxidation, leading to limited yields of CH_3OH with a large amount of CO_2 formed at high conversions.[4] The nonpolar nature of the C–H bonds of methane also inhibits its reactivity.

In the 1970s, Shilov and co-workers discovered a $Pt^{II}Cl_4^{2-}$/$Pt^{IV}Cl_6^{2-}$ system that catalyzes the oxidation of methane to methanol and/or methyl chloride with some selectivity, but this catalyst is limited by issues of catalyst stability, oxidant scope, and rate.[5] In the years since the discovery of the Shilov catalytic process, many ligand frameworks have been explored for the Pt system,[6] and efforts have been made to extend the cycle to metals such as Pd,[7] Ir,[8] Rh,[8a,9] and others.[10]

We recently conducted an ab initio screening of rhodium complexes with various ligands in the search for potential methane oxidation catalysts in trifluoroacetic acid (TFAH).[9j] Although we were inspired by Shilov and co-workers' Pt^{II}/Pt^{IV} cycle, we expanded our search with Rh to include three possible cycles, as shown in Scheme 1.

In Scheme 1, starting from an inorganic Rh^{III} resting state (**1**), we investigated the C–H activation of methane following the displacement of a TFAH solvent molecule (**2**$^+$) to form a Rh^{III}–methyl organometallic species (**3**). Starting with (**3**), there are several pathways to functionalization:

III-I: S_N2 attack (**4**$^+$) by the conjugate base of the solvent to form methyl trifluoroacetate and a Rh^I species (**5**), which is reoxidized to the inorganic Rh^{III} resting state (**1**);

III-II: S_R2 attack (**6**$^+$) by the metal–oxo species $Cl_3V{=}O$ to form a vanadium–methoxy and a Rh^{II} species (**7**) via methyl radical transfer. Both the V and Rh complexes are then reoxi-

[a] R. Fu, R. J. Nielsen, W. A. Goddard III
Materials and Process Simulation Center
California Institute of Technology
Pasadena, California 91125 (USA)
E-mail: wag@wag.caltech.edu

[b] M. E. O'Reilly, T. B. Gunnoe
Department of Chemistry
University of Virginia
Charlottesville, Virginia 22904 (USA)
E-mail: tbg7h@eservices.virginia.edu

Supporting information for this article is available on the WWW under http://dx.doi.org/10.1002/chem.201405460.

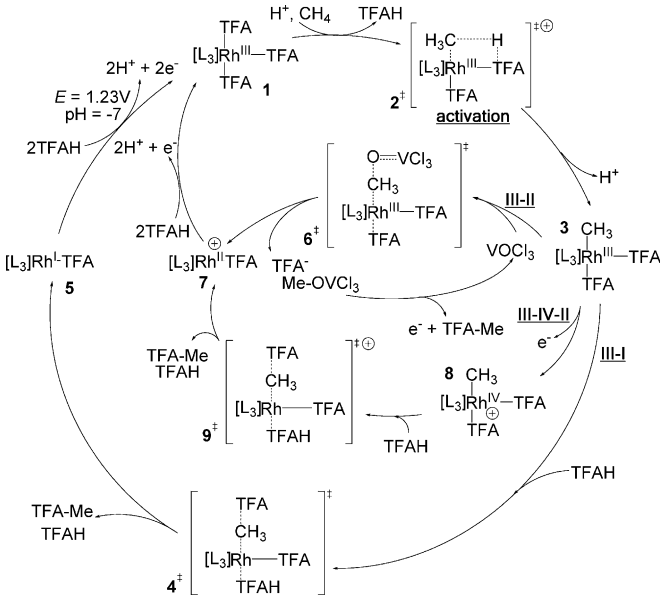

Scheme 1. Hypothetical catalytic cycles for the activation and functionalization of methane in trifluoroacetic acid (TFAH). This shows several potential routes, including Rh^{III-I}, Rh^{III-II}, and $Rh^{III-IV-II}$ cycles, which are further described in the text. [L_3] may represent a three-coordinate neutral ligand, or alternatively a two-coordinate neutral ligand and a TFAH ligand.

dized by one electron to the metal–oxo species, methanol, and the inorganic Rh^{III} resting state (**1**). Here, $OVCl_3$ was used as a model metal–oxo capable of one-electron reduction, even though it would likely hydrolyze in acidic solvents.[11] We are developing stable metal–oxo reagents optimized for this reaction mechanism and use $OVCl_3$ here as a simple model for computational studies;

III-IV-II: Oxidation to a Rh^{IV} species (**8**) followed by S_N2 attack (**9**‡) generating a Rh^{II} species (**7**), which is then further oxidized back to the Rh^{III} resting state (**1**).

In all cases, the energy of oxidation (i.e., Rh^{I} and Rh^{II} to Rh^{III} species; Rh^{III} to Rh^{IV} species) was calculated assuming a potential of 1.23 V versus SHE (standard hydrogen electrode). However, in practice it may be necessary to use intermediate oxidants as well, although that is beyond the scope of this study.

It is clear from Scheme 1 that the criteria for a successful Rh catalyst depends on two central values:

–the transition state barrier for CH_4 activation, and

–the transition state barrier for Rh–CH_3 functionalization.

A system that can proceed around any of these cycles with a global activation barrier below approximately 36 kcal mol^{-1} at 498 K is of academic interest, as transition state theory gives a turnover frequency (TOF) of roughly 1 hr^{-1} at 1 atm CH_4 for such a process. Achieving an industrially relevant TOF on the order of 1 s^{-1} requires a global barrier of 29 kcal mol^{-1}, although greater pressures of CH_4 would increase this limit.[12] The ligands we screened in our previous study and their associated barriers are reproduced in Figure S1 and Table S1, respectively, in the Supporting Information.

During the course of our previous investigation, we made the important observation that reasonable barriers in TFAH solvent were harder to find for Rh–Me functionalization than for CH_4 activation (Table S1). Hence, we designed the bis(quinolinyl)benzene (bisq^{x}) family of ligands (Figure 1) in the hopes of finding more facile S_N2 and S_R2 pathways. Ligands with a similar design have been reported by the groups of Song and Wang.[13] These ligands are expected to coordinate to Rh in

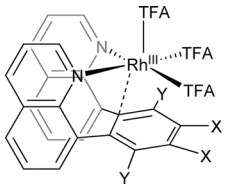

X = Y = H: bis(quinolinyl)benzene **(bisq)**
X = F, Y = H: bis(quinolinyl) difluorobenzene **(bisq^{F2})**
X = Y = F: bis(quinolinyl) tetrafluorobenzene **(bisq^{F4})**
X = Me, Y = H: bis(quinolinyl) dimethylbenzene **(bis^{Me2})**
X = Y = Me: bis(quinolinyl) tetramethylbenzene **(bisq^{Me4})**

Figure 1. The bis(quinolinyl)benzene (bisq^{x}) family of ligands, of which we investigated the base (bisq), di- and tetrafluorinated analogues (bisq^{F2}) and (bisq^{F4}), and the di- and tetramethylated analogues (bisq^{Me2}) and (bisq^{Me4}), complexed to $Rh^{III}(TFA)_3$.

a *fac*-L_3 manner with a weak η^2-benzene interaction approximately perpendicular to the N–Rh–N plane. A methyl group would then be expected to coordinate *trans* to this position, owing to the weaker *trans* effect of the benzene ring as opposed to the nitrogen donors. The η^2-benzene interaction is expected to be a better leaving group than TFA^-/TFAH, thereby lowering both the barrier and thermodynamics of functionalization. Beyond the base (bisq) ligand itself, we also investigated the di- and tetrafluorinated analogues (bisq^{F2}) and (bisq^{F4}), and the di- and tetramethylated analogues (bisq^{Me2}) and (bisq^{Me4}), to see how changing the electronics of the ligand might change its associated transition-state barriers. We are currently engaged in synthesizing and experimentally verifying these complexes. Indeed, preliminary experimental results show that Rh(bisq^{Me2}) complexes may catalyze H/D exchange with benzylic C–H bonds.[14]

Results

Scheme 2 shows the ground states of the various Rh^{III}(bisq^{x}) species in TFAH: the neutral [Rh^{III}(bisq^{x})$(TFA)_3$], the protonated [Rh^{III}(bisq^{x})$(TFA)_2$(TFAH)]$^+$ and [Rh^{III}(bisq^{x})$(TFA)_2$)]$^+$, and their relative free energies. The first point to note is that, as the (bisq^{x}) ligands are L_3, activation of methane requires first the protonation of a TFA ligand followed by its removal as TFAH to form an open coordination site. As Scheme 2 shows, as we increase the electron-withdrawing groups on (bisq^{x}) by replacing Me with H and then H with F, the resultant decrease in electron donation to the central Rh decreases the basicity of the attached TFA ligands and increases the energy of their protonated forms. The second and related point to note is that the true resting state is not consistent for all (bisq^{x}) species: the more electron-rich ligands (bisq^{Me2}) and (bisq^{Me4}) have positively charged resting states; the base ligand (bisq) exhibits near thermoneutrality between the neutral and a protonated species; and the less electron-rich ligands (bisq^{F2}) and (bisq^{F4}) prefer to be neutral. However, the energies of all species have been referenced to neutral [Rh^{III}(bisq^{x})$(TFA)_3$] for consistency. The final point to note is that the specific protonated resting

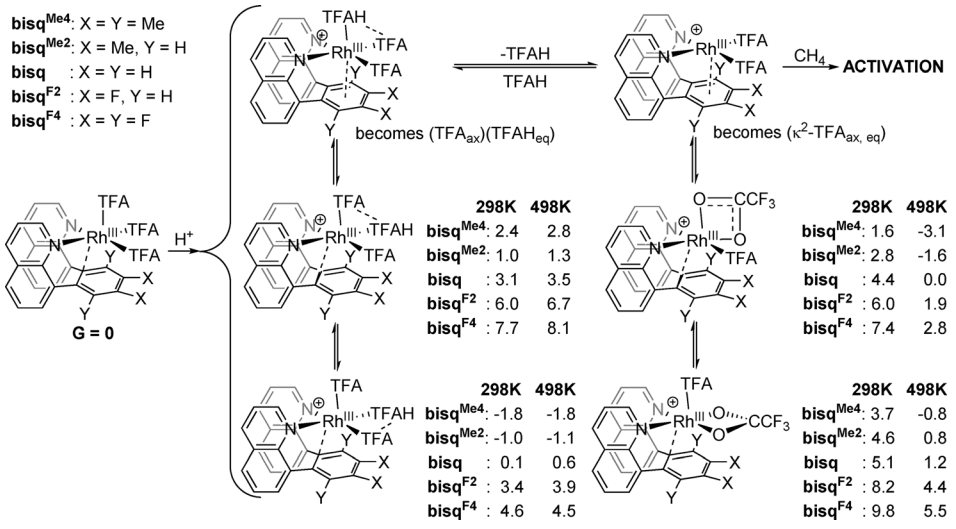

Scheme 2. The inorganic $[Rh^{III}(bisq^{x})(TFA)_3]$ species and their protonated analogues $[Rh^{III}(bisq^{x})(TFA)_2(TFAH)]^+$ and $[Rh^{III}(bisq^{x})(TFA)_2)]^+$ with their relative energies in TFAH. Both protonation and TFAH removal are necessary before methane activation can take place. All free energies are in kcal mol^{-1} and referenced to the corresponding $[Rh^{III}(bisq^{x})(TFA)_3]$ species.

It should be noted that regardless of the specific ($bisq^{x}$) ligand, the lowest energy methane activation transition state is $[Rh^{III}(bisq^{x})(TFA_{ax})(Me_{eq}\cdots H\cdots TFA_{eq})]^{+\ddagger}$, which involves an equatorial approach for the methane and results in the methyl complex $[Rh^{III}(bisq^{x})(TFA_{ax})(Me_{eq})(TFAH_{eq})]^+$. However, both the neutral and protonated Rh^{III}–Me_{ax} species are lower in energy than their equatorial counterparts. We assume that interconversion between the Rh^{III}–Me_{eq} and Rh^{III}–Me_{ax} is facile owing to the lability of the TFAH and η^2-benzene ligands.

Upon examination of the methane activation transition-state energies, a general trend is

state for the more electron-rich ligands ($bisq^{Me2}$) and ($bisq^{Me4}$) depends on temperature: at 298 K $[Rh^{III}(bisq^{Mex})(TFA_{ax})(TFAH_{eq}\cdots TFA_{eq})]^+$ is favored, but at 498 K it is more advantageous to dissociate the TFAH and have $[Rh^{III}(bisq^{Mex})(\kappa^1\text{-}TFA_{eq})(\kappa^2\text{-}TFA_{ax,eq})]^+$ instead.

Scheme 3 shows the three potential methane activation transition states that may result depending on the CH_4 molecule's approach towards the open coordination site of $[Rh^{III}(bisq^{x})(TFA)_2)]^+$. The top transition state shows the result of a methane approach to an axial open coordination site, whereas the other two show the result of an equatorial approach with either the axial or equatorial TFA ligand gaining the methane's proton. The axial approach results in a $[Rh^{III}\text{–}Me_{ax}]^+$ species, whereas the equatorial approaches result in $[Rh^{III}\text{–}Me_{eq}]^+$ species, all of which may be deprotonated to form their neutral analogues. Further oxidation to Rh^{IV} species is quite uphill; hence, the **III-IV-II** functionalization pathway was not investigated for these rhodium–ligand complexes.

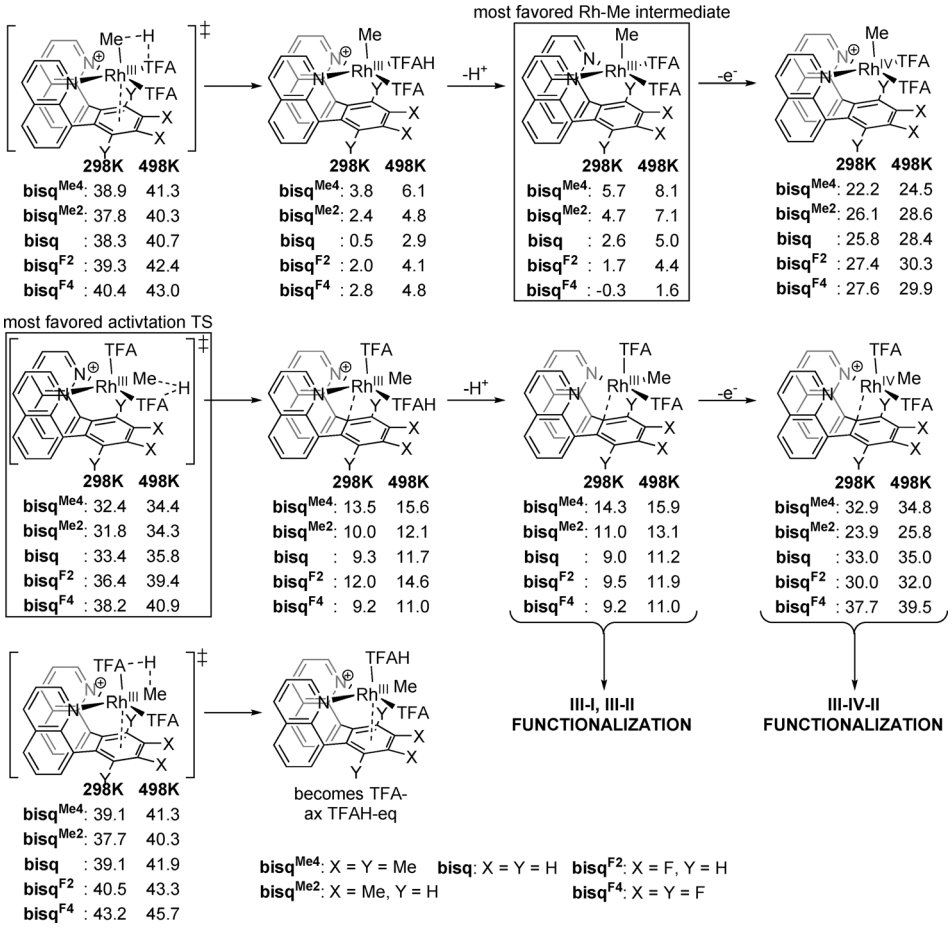

Scheme 3. The various methane activation transition states $[Rh^{III}(bisq^{x})(TFA)(Me\cdots H\cdots TFA)]^{+\ddagger}$ and their resultant $[Rh^{III}(bisq^{x})(TFA)(Me)(TFAH)]^+$ products. Ensuing deprotonation (in preparation for **III-I** and **III-II** functionalization) and oxidation (in preparation for **III-IV-II** functionalization) are also depicted. The most favored Rh–Me intermediate and activation transition state are boxed. All free energies are in kcal mol^{-1} and referenced to the corresponding $[Rh^{III}(bisq^{x})(TFA)_3]$ species.

elucidated. Increasing the electron-donating nature of groups on the (bisq^{x}) ligand results in lower activation barriers. This is opposite to that observed in the other ligand families, in which less electron-donating ligands are preferred.[15] However, a comparison of the energies of [Rh^{III}(bisq^{x})(TFA)(Me···H···TFA)]$^{+\ddagger}$ transition states with that of their protonated [Rh^{III}(bisq^{x})(TFA)$_2$(TFAH)]$^{+}$ precursors (Scheme 2) shows that the decreased activation barriers for more electron-donating ligands is *simply due to the decreased energy of protonation of the inorganic [Rh^{III}(bisq^{x})(TFA)$_3$] precursors*. This is not a factor in complexes with bidentate or anionic ligands, the resting states of which already include neutral solvent molecules. It should also be noted that for (bisq^{Me2}) and (bisq^{Me4}), the energies shown in Scheme 3 are not the full transition barriers, as they are not referenced to the ground states of those rhodium–ligand complexes. The true barriers are recorded in Table 1.

Table 1. Lowest activation and functionalization energies for the Rh(bisq^{x}) complexes in TFAH. For each entry, the first number is at 298 K and the second at 498 K. All free energies in kcal mol^{-1}.

TS type		(bisq)	(bisq^{F2})	(bisq^{F4})	(bisq^{Me2})	(bisq^{Me4})
Act.	Rh^{III} + CH$_{4ax}$	38.3	39.3	40.4	38.8	40.7
		40.7	42.4	43.0	41.9	44.4
	Rh^{III} + CH$_{4eq}$	33.4	36.4	38.2	32.8	34.3
		35.8	39.4	40.9	35.9	37.5
Funct.	+ TFA^{-} (**III-I**)	31.8	32.3	29.9	35.0	38.0
		37.8	38.4	35.0	41.9	45.5
	+ OVCl$_3$ (**III-II**)	32.0	31.8	33.4	35.7	38.9
		33.7	33.6	35.3	38.3	42.0

An examination of the energies of the lowest Rh–Me intermediate for each (bisq^{x}) ligand (Scheme 3) shows that the relative energy decreases as the electron-withdrawing nature of groups on the (bisq^{x}) ligand is increased. This is easily explained by noting that a decrease in the electron-donating power of the (bisq^{x}) ligand is expected to increase the rhodium atom's electrophilicity, and thus increase the strength of its bond with the methyl group. Indeed, for (bisq^{F4}) the Rh–Me species is slightly lower (by 0.3 kcal mol^{-1}) in energy than its [Rh^{III}(bisq^{x})(TFA)$_3$] precursor at 298 K, and the Rh–Me complex is the true resting state. However, this does not change the overall methane activation barrier.

The **III-I** S_N2 and **III-II** S_R2 functionalization pathways were investigated by searching for transition states resulting from TFA^{-}/TFAH or OVCl$_3$ attack on each Rh–Me species, axial and equatorial, neutral and positively charged for all five (bisq^{x}) ligands. A total of 65 transition-state structures are analyzed and presented in Figures S2 and S3 in the Supporting Information.

Barriers of 33.4 kcal mol^{-1} and lower at 298 K are found for (bisq) and its fluorinated analogues, thereby establishing the viability of the **III-II** pathway as well as the **III-I** pathway for methyl functionalization of the Rh^{III}(bisq^{x}) family of complexes.

Scheme 4 shows the remainder of the catalytic cycle after either **III-I** or **III-II** functionalization, and compares the two functionalization processes. Note that only the lowest energy S_N2 and S_R2 transition states are shown (see the Supporting Information for other isomers). For the **III-I** pathway, S_N2 attack by TFA^{-}/TFAH results in the formation of the MeTFA product and [Rh^{I}(bisq^{x})(TFA)(TFAH)], which is reoxidized to the starting complex [Rh^{III}(bisq^{x})(TFA)$_3$]. For the **III-II** pathway, S_R2 attack by OVCl$_3$ results in the formation of Me–OVCl$_3$ and [Rh^{II}(bisq^{x})(TFA)(TFAH)], which are also reoxidized to the starting complex [Rh^{III}(bisq^{x})(TFA)$_3$] as well as the product Me–TFA and regenerated OVCl$_3$. Either way, the final relative energy of the [Rh^{III}(bisq^{x})(TFA)$_3$] complex is −13.7 kcal mol^{-1} at 298 K, which represents a completed cycle of the overall reaction $CH_4 + TFAH \rightarrow Me\text{–}TFA + 2H^{+} + 2e^{-}$.

Finally, in addition to the **III-I** S_N2 and **III-II** S_R2 pathways, one might also envision a **I-III** pathway starting from [Rh^{I}(bisq^{x})(TFA)(TFAH)] as an alternative ground state, with CH_4 activation occurring by oxidative addition instead of concerted metal deprotonation. The results are shown in Scheme S1 in

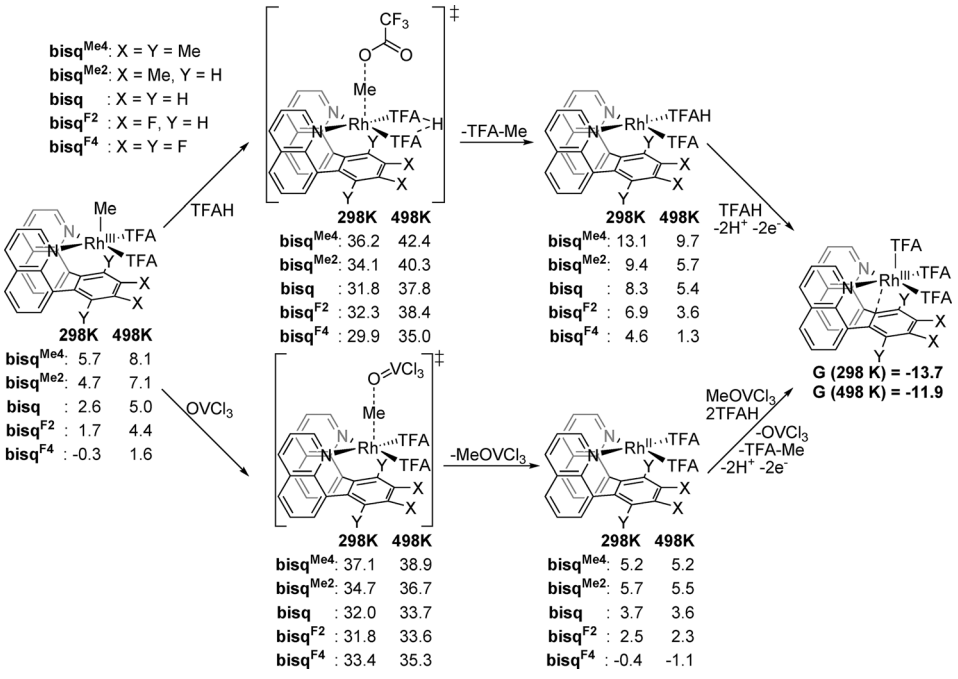

Scheme 4. Comparison of the functionalization of [Rh^{III}(bisq^{x})(Me$_{ax}$)(TFA)$_2$], the lowest energy Rh–Me species, via the **III-I** S_N2 and **III-II** S_R2 pathways, and completion of the catalytic cycle. Only the lowest functionalization transition state is shown for each pathway.

the Supporting Information. Although the oxidative addition of methane by $Rh^{I}(bisq^{x})$ species is feasible with minimum transition states of 27.9–30.6 kcal mol^{-1} depending on the particular ligand, the resulting [$Rh^{I}(bisq^{x})$(H)(Me)(TFA)] species are very uphill in energy (19.6–33.7 kcal mol^{-1}, depending on the temperature, ($bisq^{x}$) ligand, and methyl/hydride configuration (see Scheme S1 for details). Deprotonation to form a Rh^{I}–Me species was prohibitively uphill both kinetically and thermodynamically. Because of this and the fact that $Rh^{I}(bisq^{x})$ species would be less stable than their $Rh^{III}(bisq^{x})$ analogues at reaction conditions (oxidation to $Rh^{III}(bisq^{x})$ being favorable by 13.2–26.8 kcal mol^{-1}, depending on the temperature and ($bisq^{x}$) ligand; see Scheme S4 in the Supporting Information for details), we did not pursue this route further.

Discussion

The transition-state barriers for activation and functionalization of the various $Rh(bisq^{x})$ complexes are compiled in Table 1, allowing us to examine trends in barriers versus bis(quinolinyl)-benzene substituents.

By plotting the activation and transition-state energies of the various $Rh^{III}(bisq^{x})$ complexes, we can determine the ligand that is predicted to exhibit optimal activity. The results are shown in Figure 2, and they convincingly show that at both 298 K and 498 K, whether using the **III-I** or **III-II** pathway, the base ligand without functionality, **Rh^{III}(bisq), is the best choice**. In comparing the relative merits of the **III-I** and **III-II** pathways, the energies of the two transition states at 298 K are very close, within 1 kcal mol^{-1} for each ($bisq^{x}$) ligand (although, as mentioned before, ($bisq^{F4}$) appears to be an outlier). However, the energies are expected to increase at 498 K, owing to the increased entropic penalty of bringing an extra TFAH or $OVCl_3$ to the system. For the **III-I** S_N2 pathway at 498 K, this is a significant penalty of 6.0–6.2 kcal mol^{-1}, and may be enough to render functionalization inaccessible. However, for the **III-II** S_R2 pathway the entropic penalty is much less at 1.7–2.0 kcal mol^{-1}, and Rh complexes with the base (bisq) and fluorinated variants ($bisq^{F2}$) and ($bisq^{F4}$) have barriers at 35.3 kcal mol^{-1} or below. Thus it appears that **the III-II S_R2 pathway is the best choice for methyl functionalization**.

Hence, we conclude that the base Rh(bisq) rhodium–ligand complex is the best choice among the entire $Rh(bisq^{x})$ family, with an overall reaction barrier of 33.4 kcal mol^{-1} at 298 K and 35.8 kcal mol^{-1} at 498 K, when the **III-II** S_R2 functionalization pathway is used.

Although we have now ascertained that various $Rh(bisq^{x})$ complexes show reasonable barriers for the activation of methane, the BDE of the C–H bond in methanol is 9 kcal mol^{-1} weaker than that of methane. Hence, any successful catalyst must have a mechanism for preventing over-oxidation.

One potential strategy against over-oxidation that might be envisioned is product protection: if the desired product of methane activation, MeX, can be made such that it is more difficult to activate than the methane, then over-oxidation can be mitigated. Recognizing that the activation step involves donation of C–H σ-bond electron density into the Rh center, it

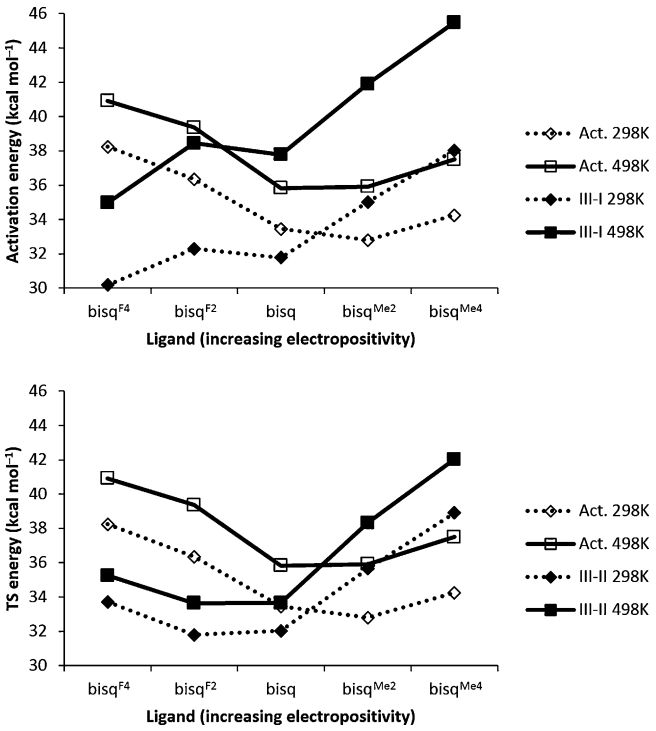

Figure 2. Top: Graph of the activation and **III-I** functionalization transition-state energies of the various $Rh(bisq^{x})$ complexes. The best choice at both 298 K and 498 K is the base Rh(bisq) complex. This complex has a maximum barrier of 33.4 kcal mol^{-1} at 298 K and 37.8 kcal mol^{-1} at 498 K. The rate-determining step is methane activation at 298 K and functionalization at 498 K. Bottom: Graph of the activation and **III-II** functionalization transition-state energies of the various $Rh(bisq^{x})$ complexes. Again, the best choice at both 298 K and 498 K is the base Rh(bisq) complex. This complex has a maximum barrier of 33.4 kcal mol^{-1} at 298 K and 35.8 kcal mol^{-1} at 498 K. The rate-determining step is methane activation at both temperatures. Both: Dashed lines denote transition state energies at 298 K, and solid lines at 498 K. Outline marker shapes denote activation transition states and filled marker shapes denote functionalization transition states. The overall barrier for each particular complex is the greater of the activation and functionalization barriers.

stands to reason that having an electron-withdrawing group for X will decrease this C–H σ-bond electron density, thus destabilizing the activation transition state and raising the barrier. Hence, whereas MeOH may be easier to activate than methane owing to the electron-donating nature of the hydroxyl group, an alternative X such as trifluoroacetate or bisulfate would render MeX harder to activate. This strategy already has been successfully utilized.[6, 9j, 16] Indeed, this strategy for product protection is also applicable to radicals, which are by nature electron deficient.[17]

Product protection studies were carried out for the $Rh(bisq^{x})$ family of rhodium–ligand complexes. The results are summarized in Figure 3. In general, the product protection $\Delta\Delta G^{\ddagger}$ energy ranges from 3.1–6.7 kcal mol^{-1} at 298 K, but improves significantly by an additional 3.8–4.2 kcal mol^{-1} at 498 K.

These product protection $\Delta\Delta G^{\ddagger}$ energies are comparable to previous work done by Owen et al.[18] They are somewhat lower than the 14 kcal mol^{-1} product protection $\Delta\Delta G^{\ddagger}$ for CH_3OSO_3H/CH_4 reported by Ahlquist et al. on the Catalytica-Periana bipyrimidine Pt catalyst, in which formation of the bi-

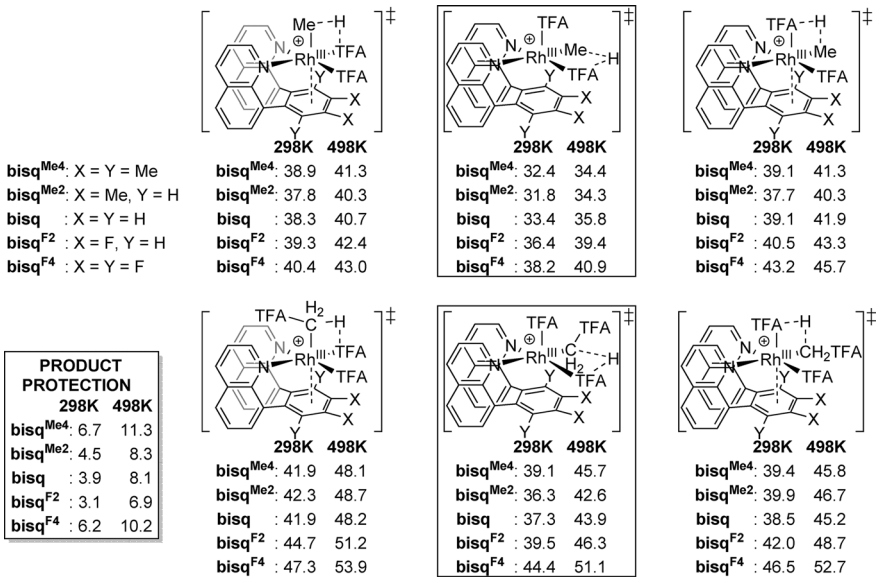

Figure 3. Comparison of the activation states of methane and methyl trifluoroacetate by the Rh(bisq^x) family of complexes, showing the product protection afforded. The most favored isomer of each type of activation is boxed. The overall product protection $\Delta\Delta G^{\ddagger}$ energies are also shown in a box to the left. All free energies are in kcal mol^{-1} and relative to the resting state.

sulfate ester is driven by the fuming sulfuric acid solvent.[19] However, a key advantage of using TFAH as the solvent in our system is the volatility of CH_3TFA (boiling point 43 °C) relative to the nonvolatile CH_3OSO_3H. Increasing selectivity without solely relying on esterification and the electrophilicity of the metal is still an important area of research, and future work may also incorporate other strategies such as hydrophobic side groups to encourage methane selectivity.

Conclusion

We have designed the Rh^{III}(bisq^x) family of complexes as a potential catalyst for methane activation and oxidative functionalization. We have found that adding electron-donating methyl groups to the ligand decreases methane activation barriers, whereas adding electron-withdrawing fluorine atoms decreases the Rh–Me functionalization barriers. The unadorned (bisq) ligand offers the best compromise in activation and functionalization. We have found, compared to our previous ligand screen work, that requiring one coordination site to be a weak η^2-benzene interaction facilitates functionalization on a methyl group *trans* to it. Experimental results show that Rh(bisq^{Me2}) complexes may catalyze H/D exchange with benzylic C–H bonds.[14] We are currently preparing and experimentally probing C–H activation and functionalization with this class of complexes. It can also be anticipated that future design of ligands may incorporate both concepts, with a weak interaction as well as an anionic or bidentate ligand, so that both activation barriers can be easily predicted and functionalization barriers minimized.

Experimental Section

All quantum mechanical calculations were carried out using the Jaguar software version 7.6 developed by Schrödinger, Inc.[20] Geometry optimizations were carried out on initial guess structures, and vibrational frequencies were gathered to confirm the optimized geometries as intermediates or transition states and to construct a free-energy profile. Solvation energies were calculated using the PBF Poisson–Boltzmann implicit continuum solvation model in Jaguar, with a dielectric constant of 8.55 and a probe radius of 2.451 Å for TFAH.[21]

Geometry optimization and vibrational data were calculated using the B3LYP density functional[22] with a smaller basis set, whereas single point gas-phase and solvated energies were calculated using the M06 functional[23] and a larger basis set. Here the "smaller basis set" consists of a modified double-ζ Los Alamos basis set and pseudopotential,[24] and the 6–31G** basis set[25] for the other atoms; whereas the "larger basis set" consists of the triple-ζ Los Alamos basis set and pseudopotential (LACV3P**++) modified to include *f* functions and diffuse functions for rhodium,[26] and the 6–311G**++ basis set for the other atoms.[27] For orbital analysis, the Pipek–Mezey localization procedure was used.[28]

Rather than specify a particular chemical oxidant, we adopted a consistent electrostatic potential for electrons to determine the free-energy changes of redox reactions. A value of 1.23 V versus SHE was adopted for models in trifluoroacetic acid. The free energy of the electron was then calculated using the equation $G = -F(E + 4.28\ \mathrm{V})$ where 4.28 V represents the absolute potential of the SHE reference.[29] The free energy of the proton was taken as −260 kcal mol^{-1} in TFAH.[30] The free energy for each molecular species in solution was calculated using the formula $G = E_{gas} + \Delta G_{solv} + \mathrm{ZPE} + H_{vib} + 6kT - T[S_{vib} + 0.54(S_{trans} + S_{rot} - 14.3\ \mathrm{e.u.}) + 7.98\ \mathrm{e.u.}]$, where the last term is an empirical approximation of the change in the translational and rotational entropy of the molecule between the gas phase and the solution phase (due to the finite librational frequencies) derived from Wertz.[31] For gas-phase molecules (methane, methyl trifluoroacetate at 498.15 K), we assumed that equilibration between the dissolved gas and the headspace occurred at a much faster timescale than the reactions in question, leading to $\Delta G_{gas\rightarrow solv} = 0$. Thus, the free energy of such gas molecules can be simply calculated using the formula $G = G_{gas} = E_{gas} + \mathrm{ZPE} + H_{tot} - TS_{tot}$.

For pure liquids (e.g., trifluoroacetic acid), the Gibbs free energy was calculated using the formula $G_{liquid} = E_{gas} + \mathrm{ZPE} + H_{tot} - TS_{tot} + \Delta G_{gas\rightarrow liquid}$, where $\Delta G_{gas\rightarrow liquid} = G_{liquid} - G_{gas}(1\ \mathrm{atm})$ is the free energy of condensation to liquid from 1 atm gas. We can solve for this by noting that $\Delta G_{gas\rightarrow liquid} = \Delta G_{exp} + \Delta G_{gas\rightarrow solv}$, where $\Delta G_{exp} = G_{gas}(P) - G_{gas}(1\ \mathrm{atm})$ is the expansion of the gas from 1 atm to the vapor pressure *P*, and $\Delta G_{gas\rightarrow solv}$ is the condensation of gas to liquid. As a liquid is by definition at equilibrium with its

vapor pressure, $\Delta G_{gas\rightarrow solv}=0$, and we thus have $\Delta G_{gas\rightarrow liquid}=G_{gas}(P)-G_{gas}(1\ atm)=RT\ln[P/(1\ atm)]$.

We can find the vapor pressure P at a given temperature by using the Antoine Equation: $\log_{10}P=A-B/(C+T)$, where the empirical parameters A, B, and C were taken to be 3.33963, 1267.252, and −52.958, respectively, which were set so that the calculated P is in bar.[32]

The S_R2 attack involving OV^VCl_3 converts two singlets to two doublets, and hence the transition states feature spin contamination ($S^2>0$) while representing an overall singlet. The reported energies are upper bounds on the energy of the uncontaminated singlet wavefunction.[33] Structures that did not feature such spin contamination were considered to be transition states for an alternative S_N2 attack that forms $MeOV^{III}Cl_3^-$ and a Rh^I species, all of which were higher in energy.

Acknowledgements

This work was solely supported as part of the Center for Catalytic Hydrocarbon Functionalization, an Energy Frontier Research Center funded by the U.S. Department of Energy, Office of Science, Office of Basic Energy Sciences, under Award No. YDE-SC0001298.

Keywords: ab initio calculations · catalysis · C–H activation · methane functionalization · rhodium

[1] R. K. Pachauri, A. Reisinger, *The Fourth Assessment Report of the Intergovernmental Panel on Climate Change*, Working Group 1, Chapter 2, Geneva, Switzerland, **2007**.

[2] F. Gerner, B. Svensson, S. Djumena, *Gas Flaring and Venting. A Regulatory Framework and Incentives for gas Utilization, Public Policy for Private Sector Journal,* No. 279, World Bank, **2004**.

[3] W.-H. Cheng, H. H. Kung, *Methanol Production and Use*, Marcel Dekker, New York, NY, **1994**, pp. 283–317.

[4] a) J. A. Labinger, J. E. Bercaw, *Nature* **2002**, *417*, 507–514; b) R. H. Crabtree, *J. Chem. Soc. Dalton Trans.* **2001**, 2437–2450; c) J. A. Labinger, *Fuel Process. Technol.* **1995**, *42*, 325–338; d) J. A. Labinger, *J. Mol. Catal. A* **2004**, *220*, 27–35.

[5] a) N. F. Goldshlegger, M. B. Tyabin, A. E. Shilov, A. A. Shteinman, *Zh. Fiz. Khim.* **1969**, *43*, 2174–2175; b) N. F. Goldshlegger, V. V. Eskova, A. E. Shilov, A. A. Shteinman, *Zh. Fiz. Khim.* **1972**, *46*, 1353–1354; c) A. E. Shilov, G. B. Shul'pin, *Activation and Catalytic Reactions of Saturated Hydrocarbons in the Presence of Metal Complexes*, Kluwer Academic Publishers, Dordrecht, **2000**; pp. 259–317.

[6] R. A. Periana, D. J. Taube, E. R. Evitt, D. G. Loffler, P. R. Wentrcek, G. Voss, T. Masuda, *Science* **1993**, *259*, 340–343.

[7] a) M. Muehlhofer, T. Strassner, W. A. Hermann, *Angew. Chem. Int. Ed.* **2002**, *41*, 1745–1747; *Angew. Chem.* **2002**, *114*, 1817–1819; b) A. Sen, M. A. Benvenuto, M. R. Lin, A. C. Hutson, N. Basickes, *J. Am. Chem. Soc.* **1994**, *116*, 998–1003.

[8] a) B. A. Arndtsen, R. G. Bergman, T. A. Mobley, T. H. Peterson, *Acc. Chem. Res.* **1995**, *28*, 154–162; b) A. G. Wong-Foy, G. Bhalla, X. Y. Liu, R. A. Periana, *J. Am. Chem. Soc.* **2003**, *125*, 14292–14293; c) J. Oxgaard, R. P. Muller, W. A. Goddard, R. A. Periana, *J. Am. Chem. Soc.* **2004**, *126*, 352–363; d) G. Bhalla, X. Y. Liu, J. Oxgaard, W. A. Goddard, R. A. Periana, *J. Am. Chem. Soc.* **2005**, *127*, 11372–11389; e) W. J. Tenn, K. J. H. Young, G. Bhalla, J. Oxgaard, W. A. Goddard, R. A. Periana, *J. Am. Chem. Soc.* **2005**, *127*, 14172–14173; f) G. Bhalla, R. A. Periana, *Angew. Chem. Int. Ed.* **2005**, *44*, 1540–1543; *Angew. Chem.* **2005**, *117*, 1564–1567; g) K. J. H. Young, O. A. Mironov, R. A. Periana, *Organometallics* **2007**, *26*, 2137–2140; h) K. J. H. Young, J. Oxgaard, D. H. Ess, S. K. Meier, T. Stewart, W. A. Goddard, R. A. Periana, *Chem. Commun.* **2009**, 3270–3272; i) R. Fu, J. E. Bercaw, J. A. Labinger, *Organometallics* **2011**, *30*, 6751–6765.

[9] a) S. K. Hanson, D. M. Heinekey, K. I. Goldberg, *Organometallics* **2008**, *27*, 1454–1463; b) M. E. Evans, W. D. Jones, *Organometallics* **2011**, *30*, 3371–3377; c) J. J. Zakzeski, A. T. Bell, *J. Mol. Catal. A* **2007**, *276*, 8–16; d) X. X. Zhang, B. B. Wayland, *J. Am. Chem. Soc.* **1994**, *116*, 7897–7898; e) W. J. Tenn, B. L. Conley, S. M. Bischof, R. A. Periana, *J. Organomet. Chem.* **2011**, *696*, 551–558; f) J. L. Rhinehart, K. A. Manbeck, S. K. Buzak, G. M. Lippa, W. W. Brennessel, K. I. Goldberg, W. D. Jones, *Organometallics* **2012**, *31*, 1943–1952; g) L. Li, W. W. Brennessel, W. D. Jones, *Organometallics* **2009**, *28*, 3492–3500; h) S. M. Kloek, D. M. Heinekey, K. I. Goldberg, *Angew. Chem. Int. Ed.* **2007**, *46*, 4736–4738; *Angew. Chem.* **2007**, *119*, 4820–4822; i) M. S. Webster-Gardiner, R. Fu, G. C. Fortman, R. J. Nielsen, T. B. Gunnoe, W. A. Goddard, *Catal. Sci. Tech.* DOI: 10.1039/c4cy00972j; j) R. Fu, R. J. Nielsen, W. A. Goddard, G. C. Fortman, T. B. Gunnoe, *ACS Catal.* **2014**, *4*, 4455–4465.

[10] a) B. G. Hashiguchi, M. M. Konnick, S. M. Bischof, S. J. Gustafson, D. Devarajan, N. Gunsalus, D. H. Ess, R. A. Periana, *Science* **2014**, *343*, 1232–1237; b) M. M. Konnick, B. G. Hashiguchi, D. Devarajan, N. C. Boaz, T. B. Gunnoe, J. T. Groves, D. H. Ess, R. A. Periana, *Angew. Chem. Int. Ed.* **2014**, *53*, 10490–10494; c) G. C. Fortman, N. C. Boaz, D. Munz, M. M. Konnick, R. A. Periana, J. T. Groves, T. B. Gunnoe, *J. Am. Chem. Soc.* **2014**, *136*, 8393–8401.

[11] M. J. Cheng, R. J. Nielsen, W. A. Goddard, *Chem. Commun.* **2014**, *50*, 10994–10996.

[12] Using $k=(RT/h)\cdot\exp(-\Delta G^{\ddagger}/RT)$.

[13] a) R. Y. Tan, P. Jia, Y. L. Rao, W. L. Jia, A. Hadzovic, Q. Yu, X. Li, D. T. Song, *Organometallics* **2008**, *27*, 6614–6622; b) S.-B. Zhao, S. Wang, *Chem. Soc. Rev.* **2010**, *39*, 3142–3156.

[14] M. E. O'Reilly, R. Fu, R. J. N. Nielsen, M. Sabat, W. A. Goddard, T. B. Gunnoe, *J. Am. Chem. Soc.* **2014**, *136*, 14690–14693.

[15] We have performed QM screening on Rh^{III} complexed with a number of different ligand systems; our data are reported in Ref [9j]. For the reader's convenience, the key results are reproduced in Figure S1 and Table S1 in the Supporting Information.

[16] L. C. Kao, A. C. Hutson, A. Sen, *J. Am. Chem. Soc.* **1991**, *113*, 700–701.

[17] T. Strassner, S. Ahrens, M. Muehlhofer, D. Munz, A. Zeller, *Eur. J. Inorg. Chem.* **2013**, *21*, 3659–3663.

[18] J. S. Owen, J. A. Labinger, J. E. Bercaw, *J. Am. Chem. Soc.* **2006**, *128*, 2005–2016.

[19] a) M. Ahlquist, R. J. Nielsen, R. A. Periana, W. A. Goddard, *J. Am. Chem. Soc.* **2009**, *131*, 17110–17115; b) R. A. Periana, D. J. Taube, S. Gamble, H. Taube, T. Satoh, H. Fujii, *Science* **1998**, *280*, 560–564.

[20] Jaguar, version 7.6, Schrödinger, LLC, New York, NY, **2007**.

[21] a) D. J. Tannor, B. Marten, R. Murphy, R. A. Friesner, D. Sitkoff, A. Nicholls, M. Ringnalda, W. A. Goddard, B. Honig, *J. Am. Chem. Soc.* **1994**, *116*, 11875–11882; b) B. Marten, K. Kim, C. Cortis, R. A. Friesner, R. B. Murphy, M. N. Ringnalda, D. Sitkoff, B. Honig, *J. Phys. Chem.* **1996**, *100*, 11775–11788.

[22] a) A. D. Becke, *Phys. Rev. A* **1988**, *38*, 3098–3100; b) A. D. Becke, *J. Chem. Phys.* **1993**, *98*, 5648–5652; c) C. T. Lee, W. T. Yang, R. G. Parr, *Phys. Rev. B* **1988**, *37*, 785–789.

[23] a) Y. Zhao, D. G. Truhlar, *Theor. Chem. Acc.* **2008**, *120*, 215–241; b) Y. Zhao, D. G. Truhlar, *Acc. Chem. Res.* **2008**, *41*, 157–167.

[24] P. J. Hay, W. R. Wadt, *J. Chem. Phys.* **1985**, *82*, 299–310.

[25] a) W. J. Hehre, R. Ditchfield, J. A. Pople, *J. Chem. Phys.* **1972**, *56*, 2257–2261; b) M. M. Francl, W. J. Pietro, W. J. Hehre, J. S. Binkley, M. S. Gordon, D. J. Defrees, J. A. Pople, *J. Chem. Phys.* **1982**, *77*, 3654–3665.

[26] J. M. L. Martin, A. Sundermann, *J. Chem. Phys.* **2001**, *114*, 3408–3420.

[27] a) T. Clark, J. Chandrasekhar, G. W. Spitznagel, P. V. Schleyer, *J. Comput. Chem.* **1983**, *4*, 294–301; b) R. Krishnan, J. S. Binkley, R. Seeger, J. A. Pople, *J. Chem. Phys.* **1980**, *72*, 650–654.

[28] J. Pipek, P. G. Mezey, *J. Chem. Phys.* **1989**, *90*, 4916–4926.

[29] C. P. Kelly, C. J. Cramer, D. G. Truhlar, *J. Phys. Chem. B* **2006**, *110*, 16066–16081.

[30] M. D. Tissandier, K. A. Cowen, W. Y. Feng, E. Gundlach, M. H. Cohen, A. D. Earhart, J. V. Coe, T. R. Tuttle, *J. Phys. Chem. A* **1998**, *102*, 7787–7794.

[31] D. H. Wertz, *J. Am. Chem. Soc.* **1980**, *102*, 5316–5322.

[32] A. Kreglewski, *Bull. Acad. Pol. Sci. Ser. Sci. Chim.* **1962**, *10*, 629–633.

[33] a) L. Noodleman, *J. Chem. Phys.* **1981**, *74*, 5737–5743; b) G. Jonkers, C. A. de Lange, L. Noodleman, E. J. Baerends, *Mol. Phys.* **1982**, *46*, 609–620; c) L. Noodleman, J. G. Norman, J. H. Osborne, A. Aizman, D. A.

Case, *J. Am. Chem. Soc.* **1985**, *107*, 3418 – 3426; d) L. Noodleman, E. R. Davidson, *Chem. Phys.* **1986**, *109*, 131 – 143; e) L. Noodleman, D. Post, E. J. Baerends, *Chem. Phys.* **1982**, *64*, 159 – 166; f) L. Noodleman, *Inorg. Chem.* **1988**, *27*, 3677 – 3679; g) L. Noodleman, D. A. Case, A. Aizman, *J. Am. Chem. Soc.* **1988**, *110*, 1001 – 1005; h) A. A. Ovchinnikov, J. K. Labanowki, *Phys. Rev. A* **1996**, *53*, 3946 – 3952; i) Y. Takahara, K. Yamaguchi, T. Fueno, *Chem. Phys. Lett.* **1989**, *157*, 211 – 216; j) Y. Kitagawa, T. Saito, M. Ito, M. Shoji, K. Koizumi, S. Yamanaka, T. Kawakami, M. Okumura, K. Yamaguchi, *Chem. Phys. Lett.* **2007**, *442*, 445 – 450; k) A. M. Mak, K. V. Lawler, M. Head-Gordon, *Chem. Phys. Lett.* **2011**, *515*, 173 – 178; l) F. Neese, *Coord. Chem. Rev.* **2009**, *253*, 526 – 563.

Received: September 29, 2014
Published online on November 21, 2014